Supporting information

Multifunctional Zn-Al Layered Double Hydroxides for Surface-Enhanced Raman Scattering and Surface-Enhanced Infrared Absorption

Yiyue Zhang,[a] Liangjing Zhang,[a] Liang Hu,[a] Shaolong Huang,[a] Zhengyuan Jin,[a] Min Zhang,[*a] Xiaoyong Huang,[b] Jianguo Lu,[c] Shuangchen Ruan,[a] Yu-Jia Zeng[*a]

[a]Shenzhen Key Laboratory of Laser Engineering, College of Optoelectronic Engineering, Shenzhen University, Shenzhen, 518060, P. R. China.

[b]Key Lab of Advanced Transducers and Intelligent Control System, Ministry of Education and Shanxi Province, College of Physics and Optoelectronics, Taiyuan University of Technology, Taiyuan 030024, P. R. China

[c]State Key Laboratory of Silicon Materials, School of Materials Science and Engineering, Zhejiang University, Hangzhou 310027, P. R. China

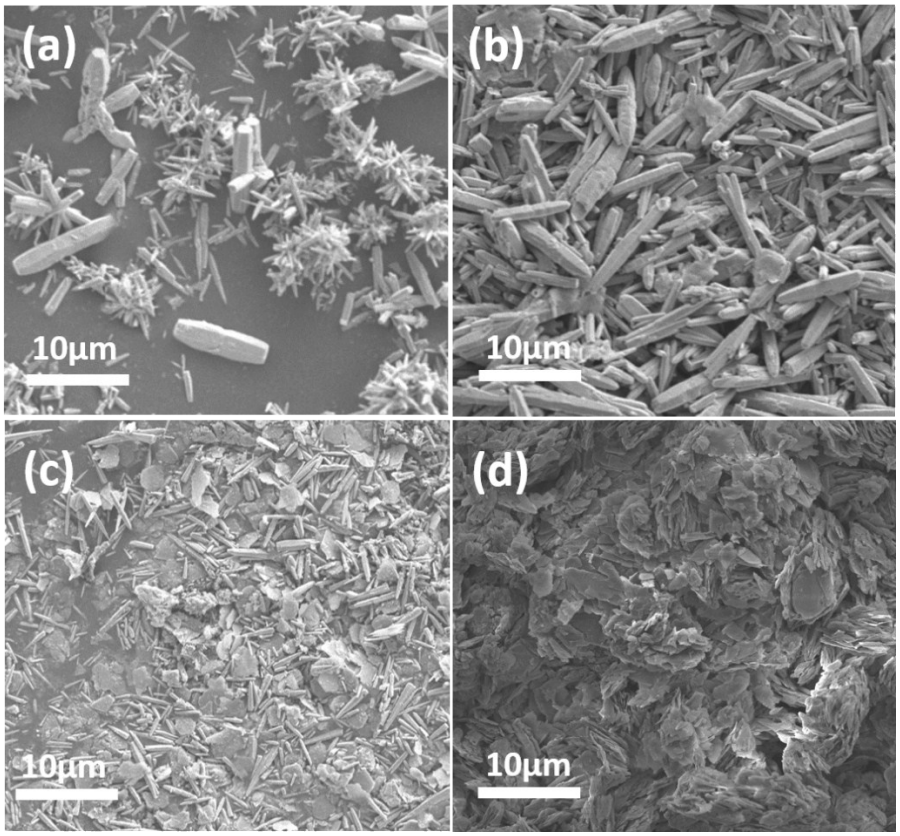

Fig. S1. (a)-(d) SEM images of the powder samples without PEG, corresponding to Al^{3+} concentration of 0, 5%, 10%, 20%, respectively.

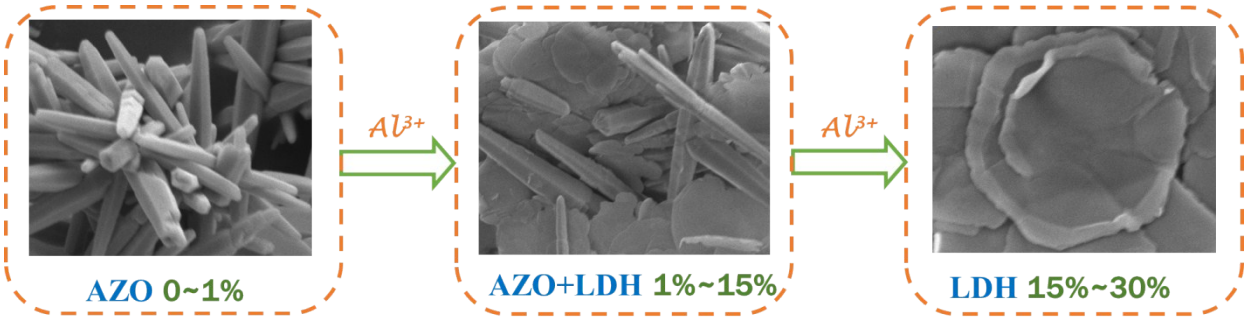

Fig. S2. SEM images of the samples at the high magnification.

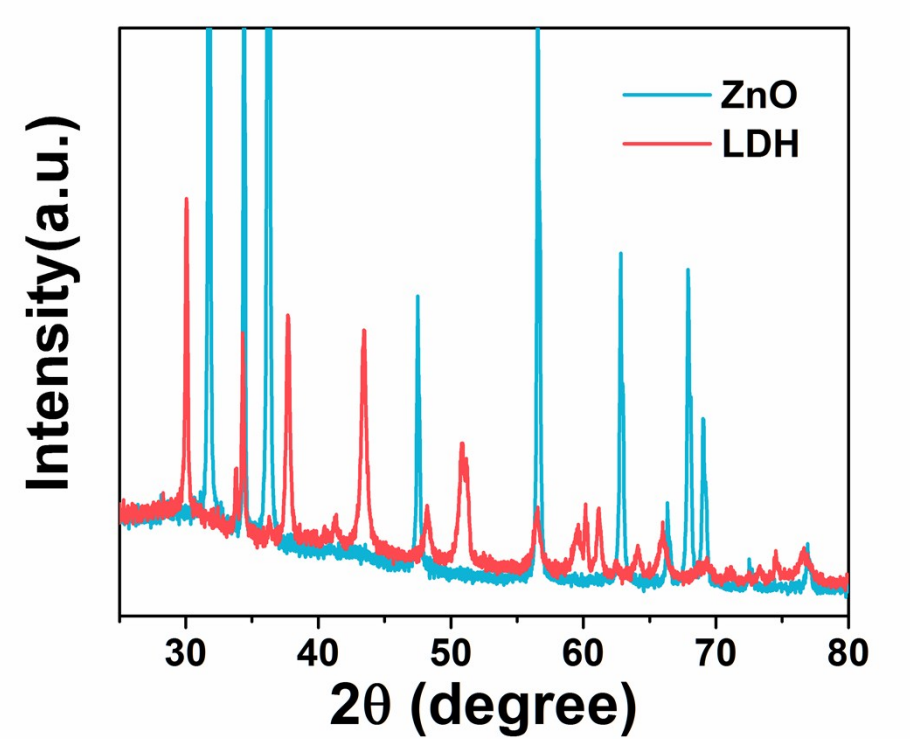

Fig. S3 XRD patterns of ZnO and Zn-Al LDH.

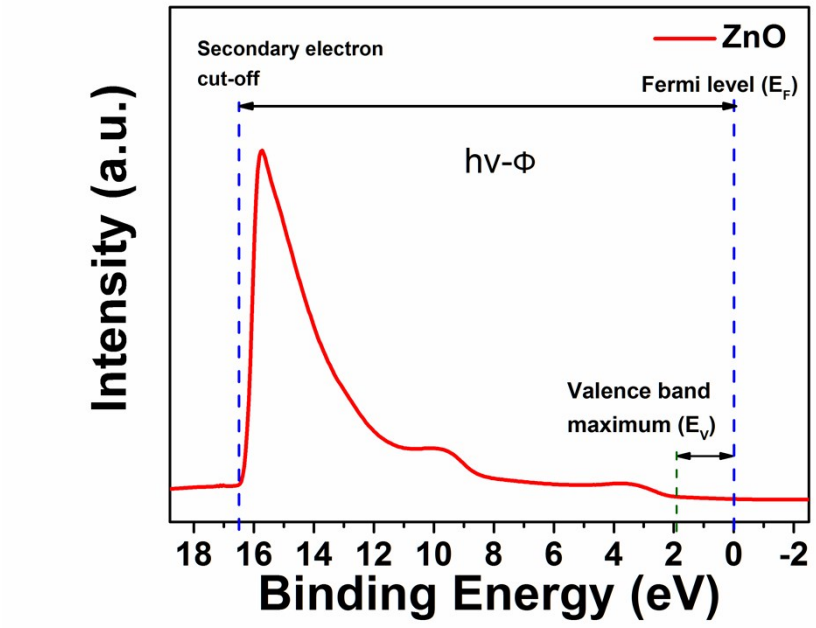

Fig. S4 Basic principles of UPS measurement for an example (pure ZnO). For a photoelectron to escape the sample surface, it must have a sufficient energy to overcome the sum of the binding energy of its initial level and the work function (Φ), where $\Phi = E_{VAC} - E_F$, and Φ is determined by the difference

between the incident photo energy and the binding energy of the secondary electron cut-off. The fixed incident photo energy is 21.2 eV, and the secondary electron cut-off represents photoelectrons with zero kinetic energy when they escape the sample surface. The difference between EF and EV is determined by the intersection of the linear portion of the spectrum near the Femi edge with the baseline.

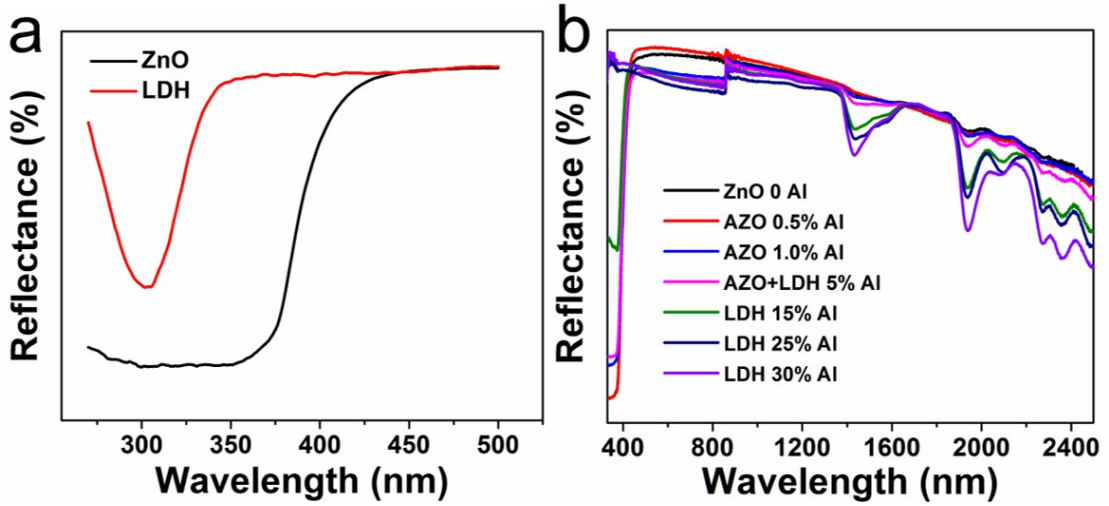

Fig. S5 UV-vis-NIR diffuse reflectance spectra of the powder samples with different Al^{3+} concentrations (0, 0.5%, 1%, 5%, 15%, 25% and 30%). The spectrum has a clear trend within this range and the nanomaterials display a broadband absorption in the NIR light range. In the region, as the amount of Al increases, the absorption peak at 1500 and 1800 nm gradually increases and the absorption peak of ZnO at 370 nm gradually decreases.

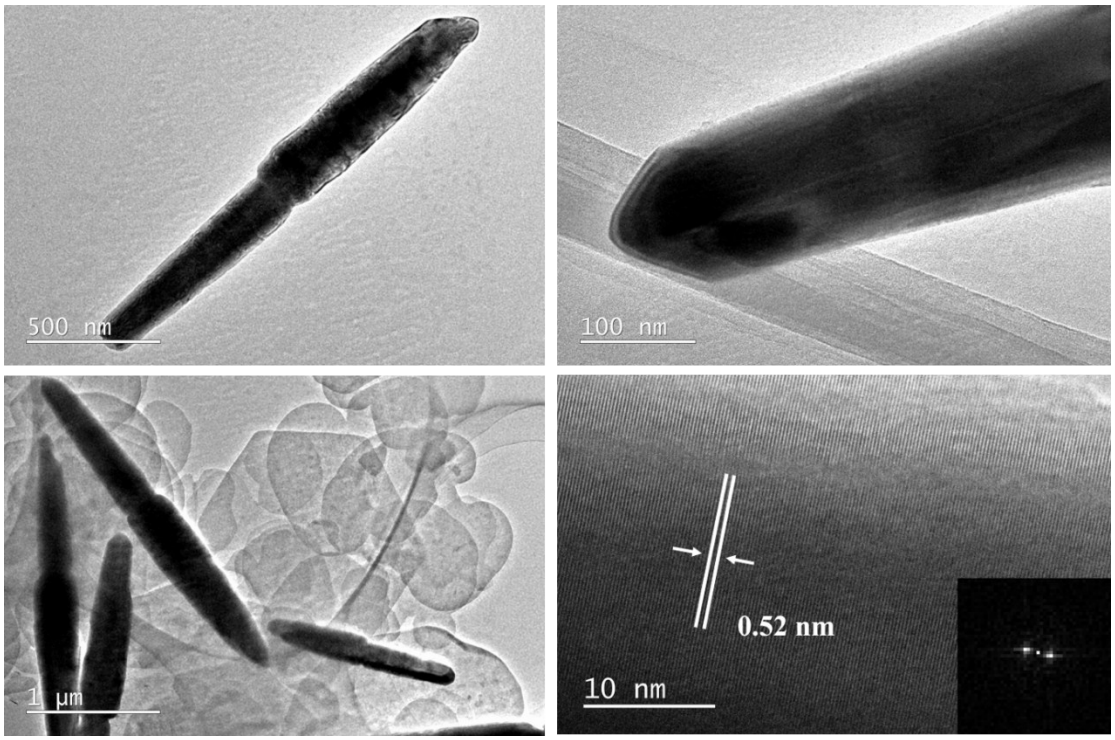

Fig. S6 (a) and (b) TEM images of the synthesized AZO (1% Al). (c) TEM images of the synthesized AZO (5% Al). (d) HRTEM images of the AZO (1% Al). (The diameter of the AZO nanorods increases from 200 nm to 400 nm with the increase of Al^{3+} ions. Meanwhile, it has a clear lattice fringe, which indicated that the samples have a good crystallinity and the inter-planar distance is measured to be 0.52 nm, corresponding to the (002) plane of rhombohedral of AZO[1, 2].)

1. S.-J. Young, C.-C. Yang and L.-T. Lai, *J. Electroanal. Chem.*, 2016, **164**, B3013-B3028.
2. M. Anbuvannan, M. Ramesh, G. Viruthagiri, N. Shanmugam and N. Kannadasan, *Spectrochim. Acta. A .* 2015, **143**, 304-308.

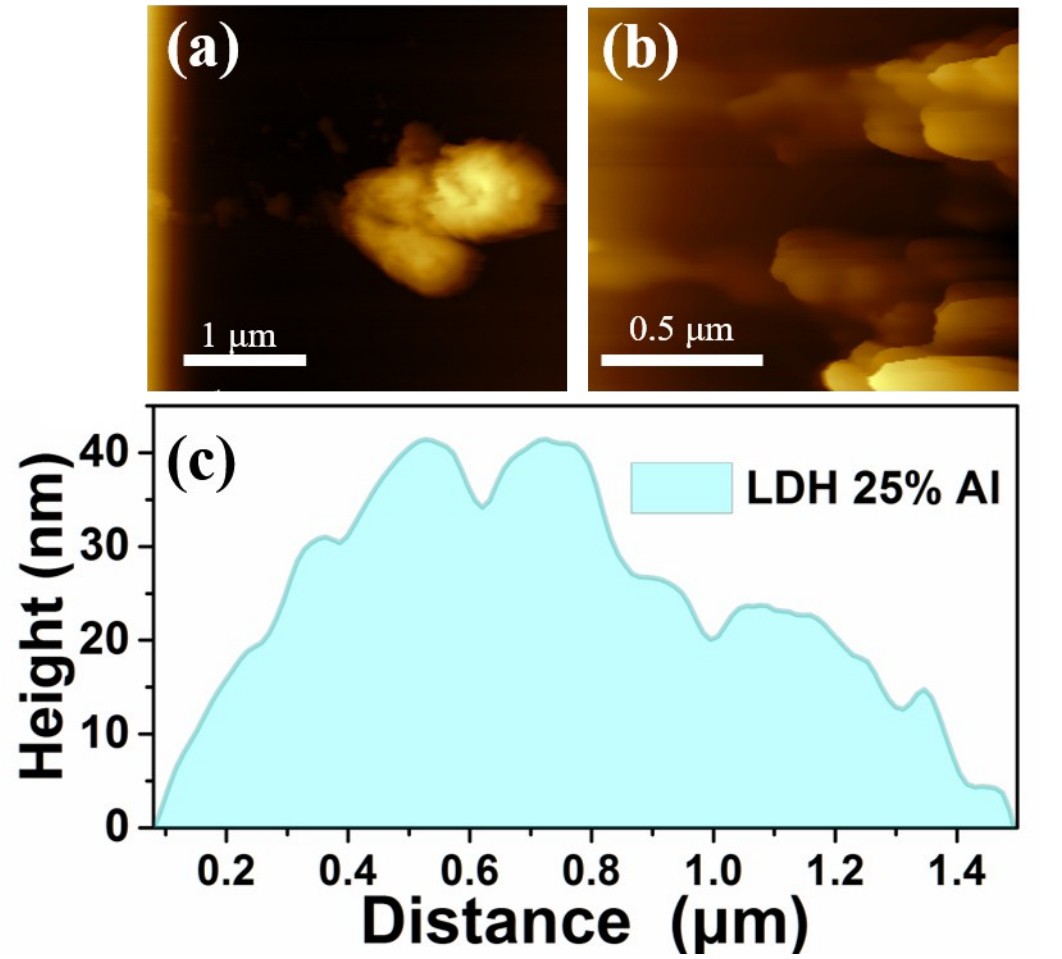

Fig. S7 (a) and (b) AFM images of the synthesized Zn-Al LDH (25% Al). (c) Height profile of the Zn-Al LDH.

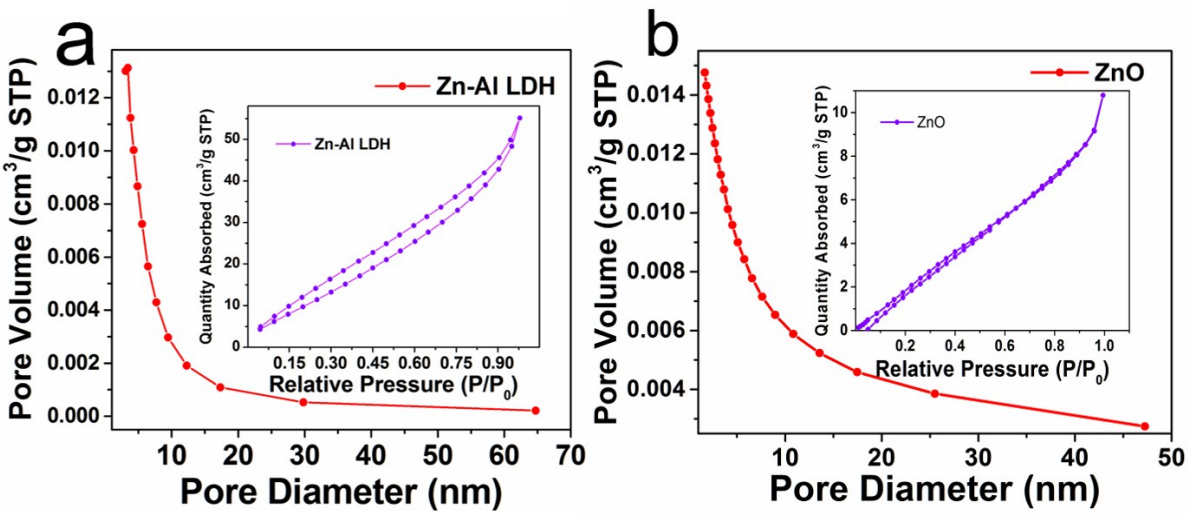

Fig. S8 BET (Brunauer-Emmett-Teller) analysis of Zn–Al LDH nanosheets.

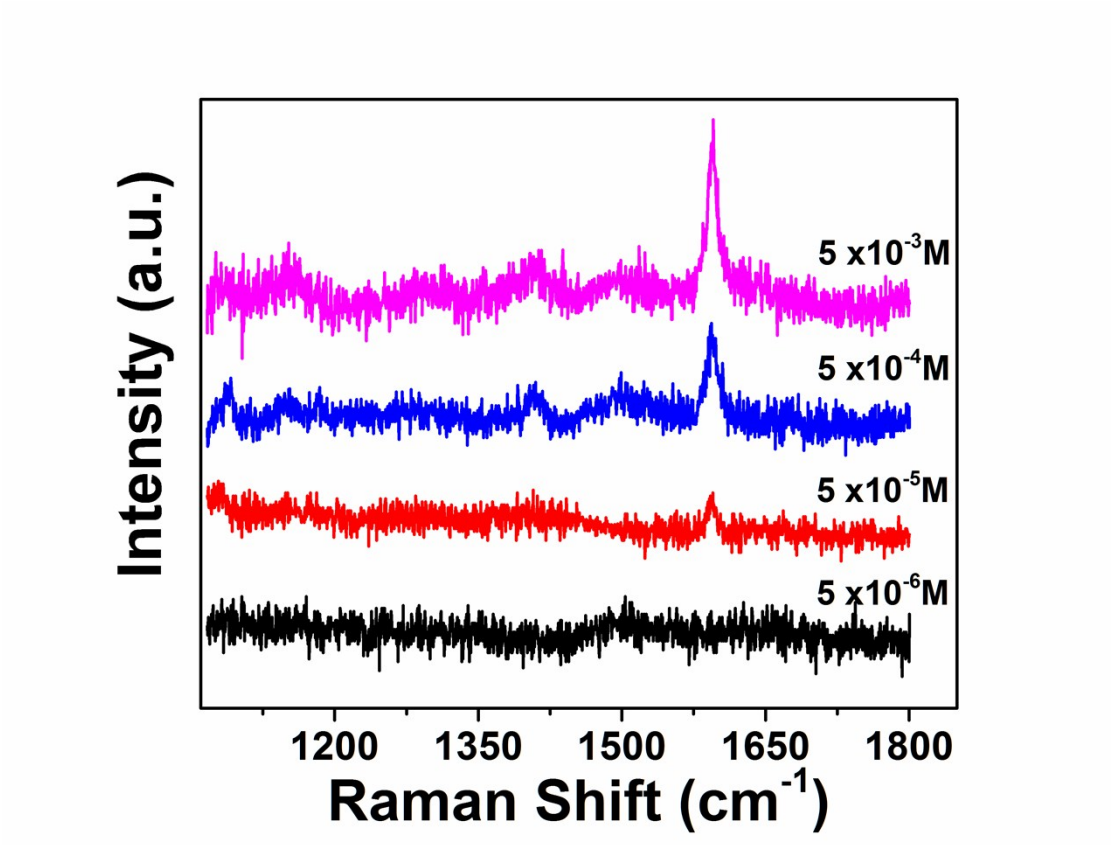

Fig. S9 SERS spectra of 4-MBA on a Zn-Al LDH substrate at different concentrations. The incident power is 5 mW, the data acquisition time is 10 s.

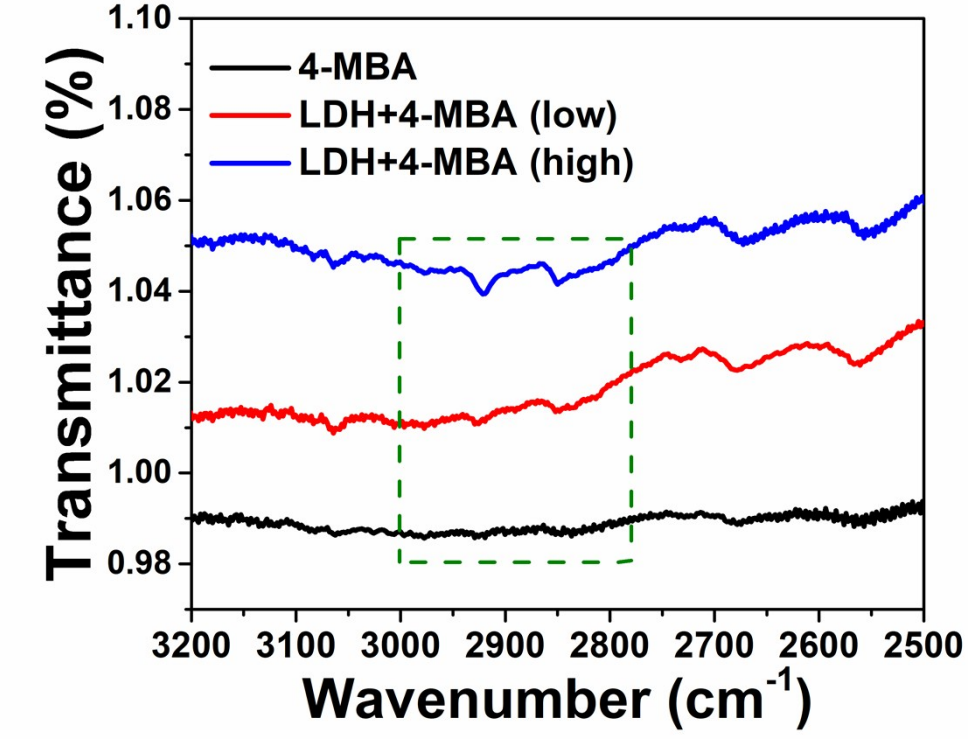

Fig.S10 FT-IR vibrational spectra of 4-MBA and LDH+4-MBA. Vibrational signals confirm the presence of "S···H–O" bridging between 4-MBA and LDH molecules. The intensity of H-bond signals is possibly related to the binding quantity about 4-MBA which relate to LDH.

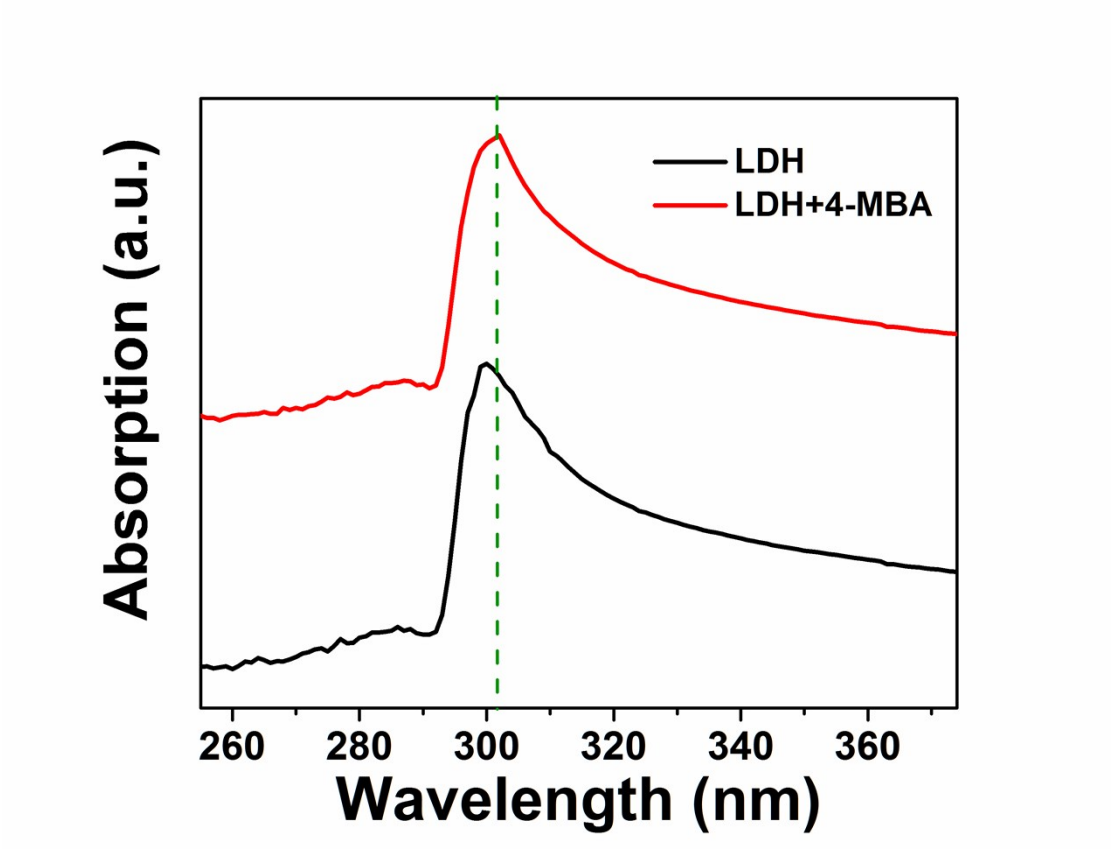

Fig.S11 UV-vis spectra of LDH and LDH+4-MBA.

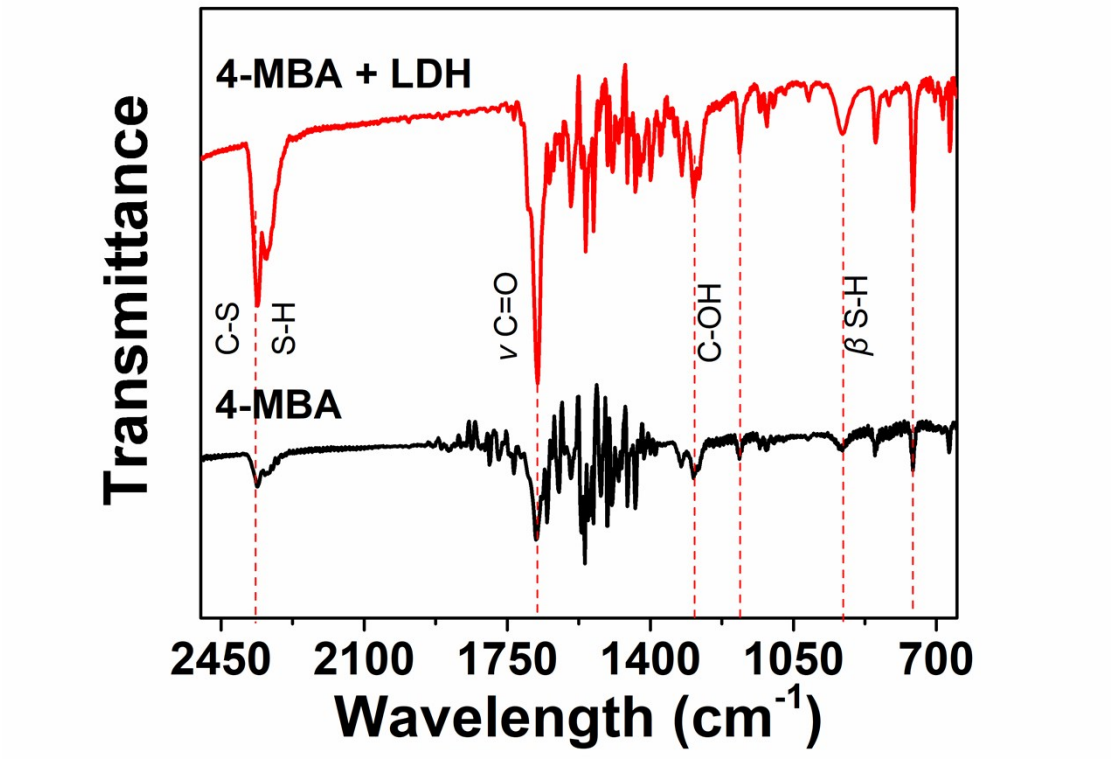

Fig. S12 SEIRA spectra of 4-MBA on a Zn-Al LDH substrate. The absorption peak at 1680 cm^{-1} corresponds to the typical stretching vibration of C=O for 4-MBA on the surface of LDH nanosheet. While the peaks at 930 cm^{-1} and 757 cm^{-1} corresponding to the bending vibration of S-H and stretching vibration of C-O, respectively. The band from 2380 cm^{-1} to 2260 cm^{-1} correspond to the C-S and S-H vibrations. Detailed vibrational information can be retrieved in the following table referenced in LANGE'S Handbook of Chemistry.

1	3450cm^{-1}	ν_{OH} from associate hydroxyls	2	2970 cm^{-1}	ν_{asCH} from $–CH_3$
3	2930 cm^{-1}	ν_{asCH} from $–CH_2–$	4	2575 cm^{-1}	ν_{asSH} from –SH
5	2364cm^{-1}	ν_{aCS} from CH_2 – S	6	2337cm^{-1}	ν_{aSH} from CH_2 – S
7	1680 cm^{-1}	$\nu_{C=O}$ from amide	8	1508 cm^{-1}	$\delta_{N–H}$ amide
9	1406 cm^{-1}	δ_{asCH} from $–CH_3$	10	1300 cm^{-1}	δ_{sCH} from –C–OH
11	930 cm^{-1}	β_{S-H} from –SH	12	757 cm^{-1}	$\delta_{C–H}$ from C–O
13	2925-2820cm^{-1}	H-bond			